Composites: Part B 69 (2015) 427–434

Contents lists available at ScienceDirect

Composites: Part B

journal homepage: www.elsevier.com/locate/compositesb

Dynamics of a functionally graded material axial bar: Spectral element modeling and analysis

Minwoo Hong, Usik Lee *

Department of Mechanical Engineering, Inha University, Inha-ro 100, Nam-gu, Incheon 402-751, Republic of Korea

ARTICLE INFO

Article history:
Received 17 March 2014
Received in revised form 7 October 2014
Accepted 8 October 2014
Available online 22 October 2014

Keywords:
A. Layered structures
B. Vibration
C. Computational modeling
C. Finite element analysis (FEA)
Functionally graded material (FGM)

ABSTRACT

Functionally graded material (FGM) bars in axial motion (hereafter called "FGM axial bars") have great potential for applications in many engineering fields. Therefore, it is important to develop a reliable mathematical model that can provide very accurate dynamic and wave propagation characteristics in FGM axial bars, especially at high frequencies. As an extension of our previous work, we present a spectral element model for a modified FGM axial bar model wherein nonuniform lateral contraction in the thickness direction is taken into account. We assume that material properties of the modified FGM axial bar model vary in the radial direction according to the power law. The performance of the proposed spectral element model is validated through comparison with solutions from a conventional finite element model, and with the results from the previous FGM axial bar model. In addition, the effects of lateral contraction on the dynamic and wave propagation characteristics in example FGM axial bars are numerically investigated.

1. Introduction

Recently, functionally graded materials (FGMs) have received considerable attention in diverse engineering fields, including the aerospace, automobile, electronics, biomedical, and defense industries. These are advanced composite materials whose properties can be spatially varied to achieve the desired structural, thermal, or electrical functions. In addition, FGMs can help reduce residual stresses or the stress concentration at an interface between two dissimilar materials, and improve the strength and toughness of a structure.

Many studies have been devoted to the static and dynamic analysis of FGM beams [1–18], FGM axial bars [19], FGM torsional bars [20], FGM plates [21], and FGM annular circular plates and disks [22,23]. In these studies, the material properties of one-dimensional (1-D) FGM structures were assumed to vary across the thickness (or radial) direction only [1–9,20], in the axial direction only [10–12,19], or in both the axial and thickness (or radial) directions [13,14]. In the literature, various solution methods have been applied to static and dynamic analyses of FGM structures; these include analytical methods [1–4,15,20–22], the Rayleigh–Ritz method [16], the modal analysis method [10,14], power series expansion methods [11,19], the differential quadrature method [14], the dynamic stiffness method [23], the finite element method (FEM) [5–9,12,17,18], and the spectral element method [24].

The FEM is a powerful computational method that can be applied to diverse complex structures including FGM structures. However, as a drawback to the FEM, a huge number of very fine meshes might be required in order to improve the accuracy of FEM solutions, especially in a high frequency regime. This can result in a significant increase in computation cost because simple polynomials that are independent of the vibrating frequency are normally used as the interpolation functions in conventional finite element formulations. In contrast to the FEM, the frequency domain spectral element method (SEM) is an exact solution method that can provide extremely accurate dynamic solutions, even at very high frequencies, by employing a minimum number of DOFs to significantly reduce the computation cost. This is because an exact dynamic stiffness matrix (often called "spectral element matrix") formulated by using frequency-dependent interpolation functions derived from exact free-wave solutions is used in the SEM as the finite element stiffness matrix [25].

FGM axial bars that take motions in the axial or longitudinal direction have great potential for the applications in many engineering fields. However, despite the aforementioned advantages of the SEM, there have been very few applications to FGM axial bars. A literature survey reveals that Maalawi [19] was the first to present analytical solutions for an FGM axial bar whose material properties vary continuously in the axial direction, and Hong et al.

* Corresponding author. Tel.: +82 32 860 7318; fax: +82 32 866 1434.
E-mail address: ulee@inha.ac.kr (U. Lee).

http://dx.doi.org/10.1016/j.compositesb.2014.10.022
1359-8368/

[26] was the first to apply the SEM to an FGM axial bar whose material properties vary in the radial direction. In [26], the lateral contraction was assumed to be uniform in the radial direction. However, physically, this may not be true for FGM bars whose material properties vary in the radial direction.

Thus, the goals of this paper are: (1) to derive modified governing equations of motion for an FGM axial bar by taking into account non-uniform lateral contraction in the thickness direction; (2) to develop a spectral element model for the modified FGM axial bar model; and (3) to investigate the effects of lateral contraction on the dynamic and wave propagation characteristics in example FGM axial bars.

2. Mathematical model: governing equations of motion

Fig. 1 shows the geometry of the uniform axisymmetric three-layer FGM axial bar (hereafter called "axial bar") considered in this study. The axial and radial coordinates are represented by x and r, respectively. It is assumed that the cross section of the FGM axial bar consists of three layers of different materials. The core ($0 \leqslant r \leqslant r_C$) and the outer layer ($r_I \leqslant r \leqslant r_O$) are made of isotropic metals, and the inner layer ($r_C \leqslant r \leqslant r_I$) is made of an FGM. We note that r_C, r_I, and r_O are the radii of the core, the inner layer, and the outer layer of the axial bar, respectively. In the following derivation, the subscripts C, I, and O denote quantities for the core, the inner layer, and the outer layer, respectively.

The displacement fields in the three layers of the axial bar are assumed to be in the following forms:

$$\begin{aligned}&\bar{u}_C(x,r,t) = u_C(x,t)\\&\bar{v}_C(x,r,t) = r\psi_C(x,t)\end{aligned} \quad (0 \leqslant r \leqslant r_C) \tag{1a}$$

$$\begin{aligned}&\bar{u}_I(x,r,t) = u_C(x,t)\\&\bar{v}_I(x,r,t) = r_C\psi_C(x,t) + (r-r_C)\psi_I(x,t)\end{aligned} \quad (r_C \leqslant r \leqslant r_I) \tag{1b}$$

$$\begin{aligned}&\bar{u}_O(x,r,t) = u_C(x,t)\\&\bar{v}_O(x,r,t) = r_C\psi_C(x,t) + (r_I-r_C)\psi_I(x,t) + (r-r_I)\psi_o(x,t)\end{aligned} \quad (r_I \leqslant r \leqslant r_O) \tag{1c}$$

where $u_C(x, t)$ is the axial displacement at the interface between the core and the inner layer, and $\psi_{(i)}(x, t)$ (i = C, I, O) represent the lateral contractions in the radial direction [27]. In this study, the axial displacements of each layer are assumed to be independent of r as the first order approximation. Note that the displacement fields in Eq. (1) fully satisfy the displacement connectivity at the interfaces among three layers. The strains in each layer can be obtained from

$$\begin{aligned}&\varepsilon_{xx}^{(i)} = \frac{\partial \bar{u}_{(i)}}{\partial x} = \frac{\partial u_C}{\partial x}, \varepsilon_{rr}^{(i)} = \frac{\partial \bar{v}_{(i)}}{\partial r}, \varepsilon_{\theta\theta}^{(i)} = \frac{\bar{v}_{(i)}}{r}\\&\gamma_{xr}^{(i)} = \frac{\partial \bar{u}_{(i)}}{\partial r} + \frac{\partial \bar{v}_{(i)}}{\partial x} = \frac{\partial u_C}{\partial r} + \frac{\partial \bar{v}_{(i)}}{\partial x}\end{aligned} \quad (i = C, I, O) \tag{2}$$

where the subscript θ denotes the circumferential direction. The constitutive relations for the elastic materials in each layer are given by

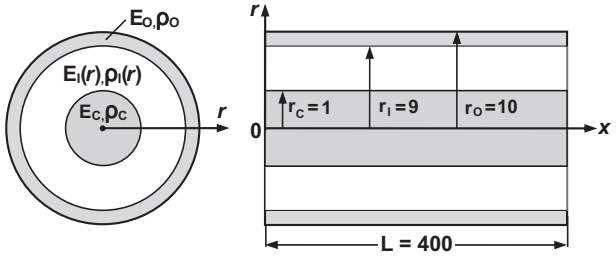

Fig. 1. Material properties and geometry of a three-layer FGM axial bar (units: mm).

$$\begin{Bmatrix}\sigma_{xx}^{(i)}\\ \sigma_{rr}^{(i)}\\ \sigma_{\theta\theta}^{(i)}\\ \tau_{xr}^{(i)}\end{Bmatrix} = \begin{bmatrix}\lambda_{(i)}+2\mu_{(i)} & \lambda_{(i)} & \lambda_{(i)} & 0\\ \lambda_{(i)} & \lambda_{(i)}+2\mu_{(i)} & \lambda_{(i)} & 0\\ \lambda_{(i)} & \lambda_{(i)} & \lambda_{(i)}+2\mu_{(i)} & 0\\ 0 & 0 & 0 & \mu_{(i)}\end{bmatrix}\begin{Bmatrix}\varepsilon_{xx}^{(i)}\\ \varepsilon_{rr}^{(i)}\\ \varepsilon_{\theta\theta}^{(i)}\\ \gamma_{xr}^{(i)}\end{Bmatrix} \tag{3}$$

where $\lambda_{(i)}$ and $\mu_{(i)}$ (i = C, I, O) are the Lamé constants, which are assumed to be constant in the core and the outer layer. In the inner layer, however, they are assumed to vary in the radial direction as follows:

$$\lambda_I(r) = \frac{E_I(r)\nu}{(1-2\nu)(1+\nu)}, \quad \mu_I(r) = \frac{E_I(r)}{2(1+\nu)} \tag{4}$$

By using the strains given by Eq. (2) and the constitutive relations given by Eq. (3), the strain energy of an axial bar element of length l can be obtained as

$$\begin{aligned}V &= \frac{1}{2}\sum_i \int_0^l \int_A \left(\sigma_{xx}^{(i)}\varepsilon_{xx}^{(i)} + \sigma_{rr}^{(i)}\varepsilon_{rr}^{(i)} + \sigma_{\theta\theta}^{(i)}\varepsilon_{\theta\theta}^{(i)} + \tau_{xr}^{(i)}\gamma_{xr}^{(i)}\right) dAdx\\ &= \frac{1}{2}\int_0^l \left(EA_{UU}u_C'^2 + EA_{CC}\psi_C'^2 + EA_{II}\psi_I'^2 + EA_{OO}\psi_O'^2\right.\\ &\quad + 2K_{CI}\psi_C'\psi_I' + 2K_{CO}\psi_C'\psi_O' + 2K_{IO}\psi_I'\psi_O' + R_{CC}\psi_C^2 + R_{II}\psi_I^2\\ &\quad + R_{OO}\psi_O^2 + 2R_{CI}\psi_C\psi_I + 2R_{CO}\psi_C\psi_O + 2R_{IO}\psi_I\psi_O + 2K_{UC}u_C'\psi_C\\ &\quad \left. + 2K_{CI}u_C'\psi_I + 2K_{CO}u_C'\psi_O\right)dx\end{aligned} \tag{5}$$

where the symbols used for effective structural properties of the axial bar are defined in Appendix A. The kinetic energy of the axial bar element can be obtained as

$$\begin{aligned}T &= \frac{1}{2}\sum_i \int_0^l \int_A \left(\rho_{(i)}\dot{\bar{u}}_{(i)}^2 + \rho_{(i)}\dot{\bar{v}}_{(i)}^2\right) dAdx\\ &= \frac{1}{2}\int_0^l \left(m_{UU}\dot{u}_C^2 + m_{CC}\dot{\psi}_C^2 + m_{II}\dot{\psi}_I^2 + m_{OO}\dot{\psi}_O^2 + 2m_{CI}\dot{\psi}_C\dot{\psi}_I\right.\\ &\quad \left. + 2m_{CO}\dot{\psi}_C\dot{\psi}_O + 2m_{IO}\dot{\psi}_I\dot{\psi}_O\right)dx\end{aligned} \tag{6}$$

where $\rho_{(i)}$ (i = C, I, O) are the mass densities, and the symbols used for effective inertia properties are defined in Appendix A. The virtual work done by a distributed axial force $q(x, t)$ acting on the outer surface of the axial bar is given by

$$\delta W = \int_0^l q(x,t)\delta\bar{u}_O dx = \int_0^l q(x,t)\delta u_C dx \tag{7}$$

In this study, the material properties of the inner layer were assumed to satisfy the power law [28] as follows:

$$\begin{aligned}E_I(r) &= (E_O - E_C)\left(\frac{r-r_C}{r_I-r_C}\right)^n + E_C\\ \rho_I(r) &= (\rho_O - \rho_C)\left(\frac{r-r_C}{r_I-r_C}\right)^n + \rho_C\end{aligned} \tag{8}$$

where n is the power law exponent.

Using Eqs. (5)–(7), the equations of motion of the axial bar can be derived from Hamilton's principle in the following forms:

$$\begin{aligned}&EA_{UU}u_C'' + K_{UC}\psi_C' + K_{UI}\psi_I' + K_{UO}\psi_O' - m_{UU}\ddot{u}_C + q(x,t) = 0\\ &EA_{CC}\psi_C'' + K_{CI}\psi_I'' + K_{CO}\psi_O'' - K_{UC}u_C' - R_{CC}\psi_C - \kappa_{CI}\psi_I - \kappa_{CO}\psi_O\\ &\quad - m_{CC}\ddot{\psi}_C - m_{CI}\ddot{\psi}_I - m_{CO}\ddot{\psi}_O = 0\\ &K_{CI}\psi_C'' + EA_{II}\psi_I'' + K_{IO}\psi_O'' - K_{UI}u_C' - \kappa_{CI}\psi_C - R_{II}\psi_I - \kappa_{IO}\psi_O\\ &\quad - m_{CI}\ddot{\psi}_C - m_{II}\ddot{\psi}_I - m_{IO}\ddot{\psi}_O = 0\\ &K_{CO}\psi_C'' + K_{IO}\psi_I'' + EA_{OO}\psi_O'' - K_{UO}u_C' - \kappa_{CO}\psi_C - \kappa_{IO}\psi_I - R_{OO}\psi_O\\ &\quad - m_{CO}\ddot{\psi}_C - m_{IO}\ddot{\psi}_I - m_{OO}\ddot{\psi}_O = 0\end{aligned} \tag{9}$$